ESRF	**Experiment title:** Oxidative removal of Fe(II), Mn(II), and As(III) by O_2, Cl_2, and MnO_4^-: Impact of chemical oxidant on the structure of Mn and Fe (oxyhydr)oxides	**Experiment number**: 26-01-1155
Beamline: BM26A	**Date of experiment**: from: 11 May, 2018 to: 15 May, 2018	**Date of report**: 28 May, 2018
Shifts: 12	**Local contact(s)**: Dipanjan Banerjee	*Received at ESRF:*

Names and affiliations of applicants (* indicates experimentalists):

Case van Genuchten (PI)*, Utrecht University

Simon Mueller*, Evides Waterbedrijf

Luuk de Waal*, KWR Watercycle Research Institute

Arslan Ahmad, KWR Watercycle Research Institute

Report:

1) Objectives. The objective of this experiment (26-01-1155) was to gain mechanistic understanding of how different ions affect the structure of co-precipitated Fe and Mn solids generated by in-situ co-oxidation of Fe(II) and Mn(II) using three different chemical oxidants often used in conventional drinking water treatment. We obtained Fe and Mn K-edge XANES and EXAFS spectra for a matrix of experimental samples produced by co-oxidizing Fe(II) and Mn(II) in solutions with systematically varied concentrations of Si, P, and Ca and by adding the oxidising O_2, HOCl and $KMnO_4$. The experimental conditions used to generate samples for Fe and Mn K-edge XAS analysis were selected to best encompass the range of chemical conditions encountered during conventional water treatment for the removal arsenic to trace levels. Knowledge of the structure of the solids formed in these experiments is not only critical to determine the pathway of arsenic oxidation and removal during co-oxidation of Fe(II) and Mn(II), but is also essential to predict the macroscopic behaviour of Fe- and Mn-containing solids in other relevant drinking water treatment processes, such as filterability during rapid sand filtration. Although we collected Fe and Mn K-edge XAS data for over 30 samples, we report only a subset of the complete sample matrix in this document.

2) Methods. Fe and Mn K-edge XAS data (XANES and EXAFS) of filtered suspensions were recorded at the DUBBLE beamline (BM26A) in transmission and fluorescence mode out to k of 13 $Å^{-1}$ (Fe) or 12 $Å^{-1}$ (Mn). Spectra were recorded at room temperature using ion chambers for transmission measurements and a 9 element solid-state Ge detector for fluorescence measurements. The X-ray beam diameter was 0.5 (vert) x 3 (horz) mm. The XANES region was measured with 0.35 eV steps, whereas step sizes of 0.05

$Å^{-1}$ were used for the EXAFS region. Two to 8 scans were collected for each sample, depending on data quality. Data reduction and preliminary analysis was performed with the SixPack software.

3) Results and Conclusions. Figure 1 shows the Fe K-edge EXAFS spectra (A) and Mn K-edge XANES spectra (B) for a key subset of experimental samples. For comparison, reference Fe-bearing (lepidocrocite, Lp, and ferrihydrite, Fh) and Mn-bearing (aqueous Mn(II), Mn_2O_3, and δ-MnO_2) materials are also given. In Figure 1, the oxidant identity for each sample is labelled first, followed by the oxyanion:Fe molar ratio and presence or absence of Ca. The results indicate that when O_2 oxidizes Fe(II) in the absence of oxyanions, Lp forms, whereas Fe(III) precipitates with a structure similar to Fh form when Fe(II) is oxidized by MnO_4^- and HOCl. The impact of co-occurring oxyanions on the structure of in-situ generated Fe(III) precipitates is most apparent when Fe(II) is oxidized by O_2, with P and Si leading to a transition from Lp-like precipitates to those that exhibit EXAFS fingerprints characteristic of Fh. In general, the entire Fe K-edge EXAFS data set, including samples not shown in Figure 1, is consistent with a decrease in structural order from lepidocrocite to poorly-ordered hydrous ferric oxide with increasing initial P and Si concentrations and when MnO_4^- and HOCl are the Fe(II) oxidant, rather than O_2.

The speciation of Mn (Figure 1B) showed more variation with chemical oxidant and solution composition than that of Fe. In the absence of oxyanions, Mn in the solid phase was dominantly trivalent when O_2 and HOCl were added, whereas MnO_4^- addition produced Mn(IV) in the solid phase. The fraction of Mn(II) increased systematically with the oxyanion:Fe ratio, particularly in the O_2 and HOCl oxidant series, with Mn(II) dominating total Mn speciation in the O_2_8Si and HOCl_8Si samples. At identical oxyanion:Fe ratios, the presence of Ca decreased the Mn(II) fraction in the solid phase, which can be explained by the competition between Ca^{2+} and Mn^{2+} for negatively-charged sorption sites created by Si and P uptake. The Mn K-edge EXAFS spectra of the same samples shown in Figure B indicate the formation of MnO_2 in the MnO_4^- sample series, whereas Mn(III)-incorporated Fe(III) precipitates with varying sorbed Mn(II) fractions formed in the O_2 and HOCl sample series.

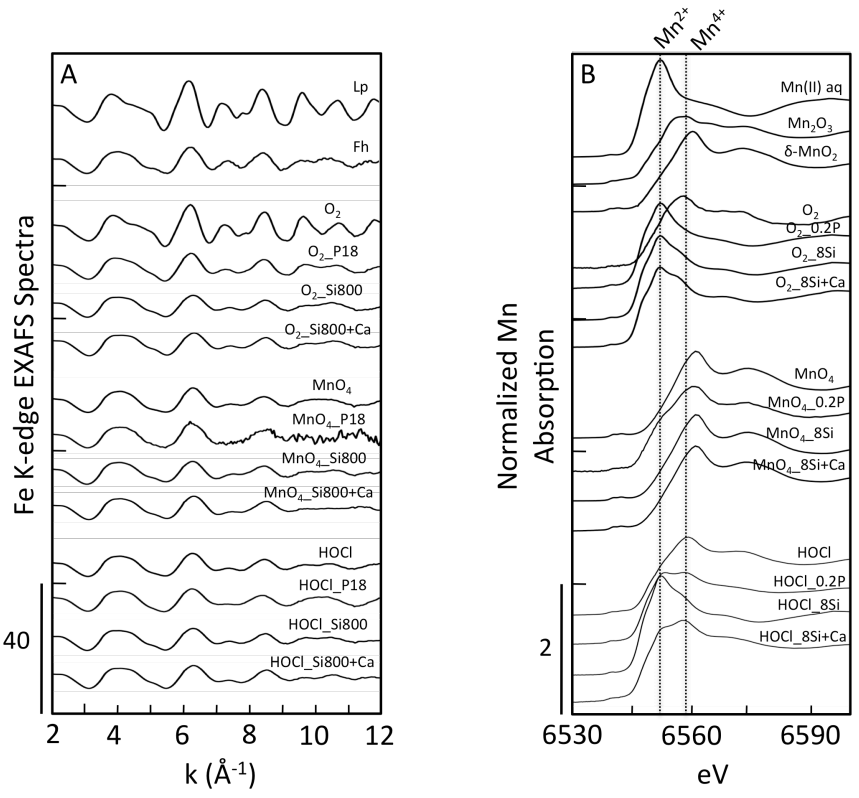

Figure 1: Fe K-edge EXAFS spectra (A) and Mn K-edge XANES spectra (B) of solids formed by Fe(II) and Mn(II) co-oxidation with O_2, MnO_4^-, and HOCl.

4) Future Experiments. We plan to investigate the oxidation and sorption of As co-precipitated with Fe and Mn (oxyhydr)oxides in identical experimental conditions as in this study. A proposal to obtain access to a synchrotron beam line with As K-edge XAS capability is currently in preparation.